# Distinct Hierarchical Alterations of Intrinsic Neural Timescales Account for Different Manifestations of Psychosis

Kenneth Wengler, PhD[1,2], Andrew Goldberg[2], George Chahine, MD[3], and Guillermo Horga, MD, PhD[1,2]

1. Department of Psychiatry, Columbia University, New York, NY, USA
2. New York State Psychiatric Institute, New York, NY, USA
3. Department of Psychiatry, Yale University, New Haven, CT, USA

Corresponding Author: Kenneth Wengler, PhD
Department of Psychiatry, Columbia University
Division of Translational Imaging, New York State Psychiatric Institute
1051 Riverside Dr, Unit 31
New York, NY 10032
Phone: 646-774-5571
Email: Kenneth.Wengler@nyspi.columbia.edu

Corresponding Author: Guillermo Horga, MD, PhD
Department of Psychiatry, Columbia University
Division of Translational Imaging, New York State Psychiatric Institute
1051 Riverside Dr, Unit 31
New York, NY 10032
Phone: 646-774-5810
Email: Guillermo.Horga@nyspi.columbia.edu

**Abstract**

Hierarchical perceptual-inference models of psychosis may provide a holistic framework for understanding the psychotic syndrome of schizophrenia, including heterogeneity in its clinical presentations. Particularly, these models may explain why positive symptoms such as hallucinations and delusions tend to cluster together yet sometimes manifest in isolation: alterations at distinct levels of the perceptual-inference hierarchy (low vs. high) may cause individual symptoms (hallucinations vs. delusions), which in turn may tend to co-occur given interdependence across hierarchical levels. Here, using a recently developed resting-state fMRI measure of intrinsic neural timescale (INT)—reflecting the time window of neural integration in a brain region and capturing hierarchical brain gradients—we aimed to test whether hallucinations and delusions are associated with distinct hierarchical alterations. First, we examined the robustness of INT and its relationship to a structural measure of neural hierarchies in 100 healthy subjects. Next, we investigated differences in INT between 127 patients with schizophrenia and 152 age- and gender-matched controls, finding that patients exhibited a widespread INT reduction. Finally, by examining INT gradients within anatomically defined hierarchies of the visual and auditory systems, we found distinct hierarchical INT alterations that scaled respectively with hallucination and delusion severity in the auditory system. Altogether and supported by simulations from a large-scale biophysical model, our results suggest (1) a global reduction of INT in schizophrenia consistent with a global reduction in excitation-inhibition ratio, and (2)

distinct hierarchical alterations associated with hallucinations and delusions that are consistent with focal increases in excitation-inhibition ratio at specific hierarchical levels.

**Keywords**
Psychosis, Intrinsic Neural Timescale, Schizophrenia, Excitation-Inhibition

## 1. Introduction

Hallucinations and delusions are burdensome symptoms that typically manifest together as the psychotic syndrome of schizophrenia. Perceptual-inference models of psychosis suggest that these symptoms result from alterations in the updating of internal models of the environment that are used to make inferences about external sensory events and their causes (1-3). These models are receiving increasing empirical support (4-9), yet current theories do not provide a satisfactory explanation for how hallucinations and delusions tend to co-occur but sometimes manifest in isolation. This suggests that these psychotic symptoms may share a common neurobiological mechanism and simultaneously depend on symptom-specific pathways.

We and others have proposed that this apparent tension may be resolved in the context of hierarchical perceptual-inference models (1, 3, 4, 10-13). One possibility is that alterations at higher levels—supporting inferences on abstract hidden states like someone's intentions—may drive delusions, and alterations at lower levels—supporting inferences about lower-level features of stimuli such as stimulus presence or absence—may drive hallucinations (2, 4, 6, 8, 14, 15). In addition to these symptom-specific pathways, alterations at any level may naturally propagate throughout the interdependent levels of the hierarchy, potentially explaining symptom co-occurrence (16). Importantly, inferential neural systems are thought to feature a hierarchical architecture of timescales that mirrors the hierarchical temporal dynamics of natural environments, where rapidly changing events are typically nested within slower changing contexts (17, 18). Thus, inferences pertaining to slower changing contexts

require neural systems with the ability to integrate information over longer periods of time, an ability consistent with the persistent neuronal activity that characterizes higher-level regions (19).

A hierarchy of neural timescales has been observed in both single-neuron recordings in non-human primates (20) and functional magnetic resonance imaging (fMRI) recordings in humans (21-25); and was reproduced using a large-scale biophysical model (16). In particular, a newly developed method based on resting-state fMRI was shown to capture a hierarchy of intrinsic neural timescales (INT), as well as alterations in psychopathology (26). Here, we specifically applied this method to test whether hallucinations and delusions are associated with distinct changes in INT at low and high levels of neural hierarchies, respectively. We hypothesized that INT at these respective levels would increase with more severe symptoms, reflecting increased neural integration of prior information in line with behavioral findings in hallucinations and delusions (4, 5, 27-29). If present, these INT changes should manifest as symptom-specific differences in hierarchical gradients.

## 2. Methods

### *2.1. Human Connectome Project Dataset*

T1w/T2w maps and resting-state fMRI data were obtained for a subset of 100 unrelated young and healthy subjects from the Human Connectome Project (HCP) WU-Minn Consortium (30) (**Supplement**). The preprocessed fMRI data were then used for estimation of INT maps in 32k Conte69 mesh surface space and in

MNI152_ICBM2009a_nlin volume space with native spatial resolution. The T1w/T2w (myelin) maps (31) in 32k Conte69 mesh surface space were used to compare functional (INT) and structural (T1w/T2w) measures of hierarchy.

### *2.2. Schizophrenia Combined Dataset*

T1w images and resting-state fMRI data were obtained for 331 healthy control subjects and 254 patients diagnosed with either schizophrenia (N = 241) or schizoaffective disorder (N = 13) from four publicly available datasets (**Supplement**). The final sample after quality-control checks consisted of 127 patients and 152 age- and gender-matched controls (**Supplement**). The preprocessed fMRI data were then used for estimation of INT maps in MNI152_ICBM2009a_nlin volume space with native spatial resolution.

Symptom severity in patients was assessed with the Positive and Negative Syndrome Scale (PANSS) (32) in the COBRE and BrainGluSchi samples, or with the Scale for the Assessment of Positive Symptoms (SAPS) (33) and the Scale for the Assessment of Negative Symptoms (SANS) (34) in the UCLA and NMorphCH samples. To appropriately combine the scores across all four samples, we chose the subset of 7 items that constituted unequivocal matches between the PANSS and SAPS/SANS (in parentheses): delusions (global rating of delusions), conceptual disorganization (global rating of positive formal thought disorder), hallucinatory behavior (global rating of hallucinations), blunted affect (global rating of affective flattening), emotional withdrawal (global rating of anhedonia/asociality), passive/apathetic social withdrawal (global rating

of avolition/apathy), lack of spontaneity and flow of conversation (global rating of alogia). PANSS scores were decreased by 1 point for all levels of severity and the severe and moderately severe levels were combined into a single level so that scoring conformed to the SAPS/SANS scale (from 0 to 5 with increasing severity).

### *2.3. Estimation of Intrinsic Neural Timescale Maps*

The preprocessed fMRI data were further processed for artifact removal (**Supplement**) and INT maps were then estimated as previously described (26). Briefly, the autocorrelation function of the fMRI signal at each voxel (or vertex) was estimated and the sum of the autocorrelation coefficients during the initial positive period was calculated. This initial positive period included all timepoints from the current timepoint (zero lag) until the timepoint immediately preceding the first lagged timepoint with a non-positive autocorrelation coefficient. To adjust for differences in temporal resolution, the sum was multiplied by the TR of the fMRI data. This product was used as an index for INT (Note that values are similar to those from an exponential fit (20); **Supplement**).

### *2.4. Statistical Analysis*

#### *2.4.1. HCP Dataset*

Based on previous work showing that lower T1w/T2w map values co-localize with higher hierarchical levels (35) and the hierarchical nature of INT (16, 20), we examined the spatial relationship between T1w/T2w and INT values. Group-averaged T1w/T2w and INT maps in surface space were parcellated using the HCP-multimodal

parcellation and separated into 6 parcel groups (36) (**Supplement**). We tested the parcel-wide spatial relationship between T1w/T2w and INT values using linear regression. The relationship between T1w/T2w and INT maps was further investigated by comparing their values within the well-defined anatomical hierarchies of the visual and auditory systems using non-parametric Spearman correlations.

To evaluate potential confounds of the INT values, we examined their relationship with age, gender, and head motion—based on mean framewise displacement (37) (FD)—using linear regression. The relationship to available cognitive measures was also explored (**Supplement**).

To estimate the reliability of the INT measure in the schizophrenia combined dataset, INT maps were calculated in volume space for the HCP dataset using timeseries of approximately the same duration as those available in the schizophrenia combined dataset (**Supplement**) and two-way random, single score intraclass correlation coefficients [ICC(2,1)] were computed (38).

*2.4.2. Schizophrenia Combined Dataset*

INT maps were parcellated into 180 cortical parcels using HCP-MMP1.0 in volumetric space (https://identifiers.org/neurovault.collection:1549) and 8 FreeSurfer (39) subcortical parcels (thalamus, caudate, putamen, pallidum, hippocampus, amygdala, nucleus accumbens, and ventral diencephalon). In an exploratory analysis, differences in INT map values between patients with schizophrenia and healthy controls were investigated using a linear-regression model ($M1_{exploratory}$) predicting INT values as

a function of diagnosis while controlling for age, gender, mean FD, and sample-acquisition site (BrainGluSchi, COBRE, NMorphCH, and UCLA). To test our hypothesis of hallucination- and delusion-specific alterations in INT, we evaluated the relationships between symptom severity and INT values using a linear-regression model ($M1_{primary}$) predicting INT with each of the 7 symptoms (hallucinations, delusions, conceptual disorganization, emotional withdrawal, social withdrawal, blunted affect, and alogia) as regressors while controlling for age, gender, mean FD, and sample-acquisition site. We did not use standard statistical parametric-mapping approaches because our main focus was on effects along hierarchical gradients not necessarily dependent on anatomical proximity.

*2.4.3. Permutation Testing*

To assess statistical significance while controlling for multiple comparisons, we used permutation tests, which provide adequate protection against false positives in fMRI analyses (40). Our main test focused on differences between hallucinations and delusions in INT gradient effects within anatomically defined hierarchies of the auditory and visual systems—reflecting symptom-specific INT alterations at different hierarchical levels. This focus was justified by the greater consistency we observed across structural and functional hierarchical indices within the auditory and visual systems (**Figure 1**) and because hallucinations in schizophrenia tend to predominate in these modalities (41, 42). Also, the auditory and visual systems, unlike the sensorimotor system, have the same number of clearly defined hierarchical levels and are thus more easily

comparable. We specifically tested our hypothesis using a linear-regression model (M2) featuring interactions of symptom-by-hierarchical-level within anatomical gradients in sensory systems. We included a symptom-by-hierarchical-level-by-sensory-system interaction to test for differences between sensory systems. Permutation tests compared observed effects [parcel-wise t-statistics of individual regression coefficients from M2 (or $M1_{exploratory}$)] to those in a null distribution obtained from 10,000 surrogate datasets in which the values of the predictor variables of interest in $M1_{primary}$ (or $M1_{exploratory}$) were randomly shuffled. Corrected *P*-values at 0.05 ('$P_{permutation}$'), two-sided, are reported.

### *2.4.4. Large-Scale Biophysical Model of Cortical Neural Timescales*

We used a computational model of macaque cortex previously shown to capture the hierarchy of neural timescales observed using electrophysiology (16). The model consists of 29 nodes with local excitatory and inhibitory pools of neurons. These nodes have both local (recurrent) and long-range connections. We then investigated alterations in excitation-inhibition (E/I) ratios by changing the strength of recurrent connections to recapitulate our *in vivo* observations. Complete details are provided in the **Supplement**.

**Table 1**: **Participant Characteristics**

| Variable | Healthy Controls | | | | | Schizophrenia Subjects | | | | |
|---|---|---|---|---|---|---|---|---|---|---|
| | BGS | COBRE | NMCH | UCLA | All | BGS | COBRE | NMCH | UCLA | All |
| N | 24 | 42 | 25 | 67 | 158 | 40 | 31 | 26 | 30 | 127 |
| Age, mean (SD), y | 36.0 (13.1) | 33.9 (10.4) | 29.8 (7.2) | 32.3 (8.5) | 32.9 (9.7) | 31.1 (12.6) | 30.5 (11.9) | 30.5 (6.2) | 35.0 (8.9) | 31.8 (10.6) |
| Male sex, No. (%) | 22 (92) | 34 (81) | 16 (64) | 54 (81) | 126 (80) | 38 (95) | 26 (84) | 19 (73) | 22 (73) | 105 (83) |
| Framewise Displacement, mean (SD), mm | 0.15 (0.04) | 0.14 (0.05) | 0.14 (0.11) | 0.10 (0.04) | 0.13 (0.06)* | 0.16 (0.06) | 0.17 (0.06) | 0.12 (0.06) | 0.13 (0.04) | 0.15 (0.06) |
| Delusion Score, mean (SD) | NA | NA | NA | NA | NA | 2.3 (1.6) | 1.7 (1.5) | 3.2 (1.9) | 2.5 (1.4) | 2.4 (1.7) |
| Hallucination Score, mean (SD) | NA | NA | NA | NA | NA | 2.1 (1.6) | 1.7 (1.4) | 2.9 (2.0) | 2.2 (1.6) | 2.2 (1.7) |
| Conceptual Disorganization Score, mean (SD) | NA | NA | NA | NA | NA | 0.9 (1.3) | 0.6 (1.0) | 2.0 (1.6) | 1.4 (1.4) | 1.2 (1.4) |
| Emotional Withdrawal Score, mean (SD) | NA | NA | NA | NA | NA | 1.8 (1.2) | 1.2 (1.3) | 3.4 (1.7) | 2.3 (1.5) | 2.1 (1.6) |
| Social Withdrawal Score, mean (SD) | NA | NA | NA | NA | NA | 1.8 (1.4) | 1.3 (1.4) | 3.2 (1.7) | 2.7 (1.6) | 2.2 (1.6) |
| Blunted Affect Score, mean (SD) | NA | NA | NA | NA | NA | 1.8 (1.6) | 1.6 (1.5) | 3.3 (1.6) | 1.1 (1.1) | 1.9 (1.6) |
| Alogia Score, mean (SD) | NA | NA | NA | NA | NA | 1.3 (1.6) | 1.2 (1.4) | 2.1 (1.7) | 0.9 (1.6) | 1.3 (1.6) |

BGS, BrainGluSchi; NMCH, NMorphCH; SD, standard deviation

## 3. Results

### *3.1. Evaluation of Intrinsic Neural Timescales versus Structural and Anatomical Hierarchies in the HCP Dataset*

We first sought to describe the relationship between INT (26), an index of functional hierarchy (16, 20), and the T1w/T2w index of structural hierarchy (35) (**Figure 1**). Consistent with prior empirical and theoretical work (16, 43), we did not observe a systematic function-structure relationship across the whole brain **(Figure 1E**;

**Supplement**). Given the heterogeneity in INT values across parcel groups, we investigated the relationship between T1w/T2w and INT along the well-defined anatomical hierarchies within the auditory and visual systems (36, 44-48), which should exhibit a closer structure-function relationship (43). Here, we indeed observed a clear relationship between T1w/T2w and INT values (auditory: $\rho$ = -0.71, $P$ = 0.04; visual: $\rho$ = -0.89, $P$ = 0.01; **Figure 1F**; sensorimotor: $\rho$ = -0.89, $P$ = 0.03; **Supplement**).

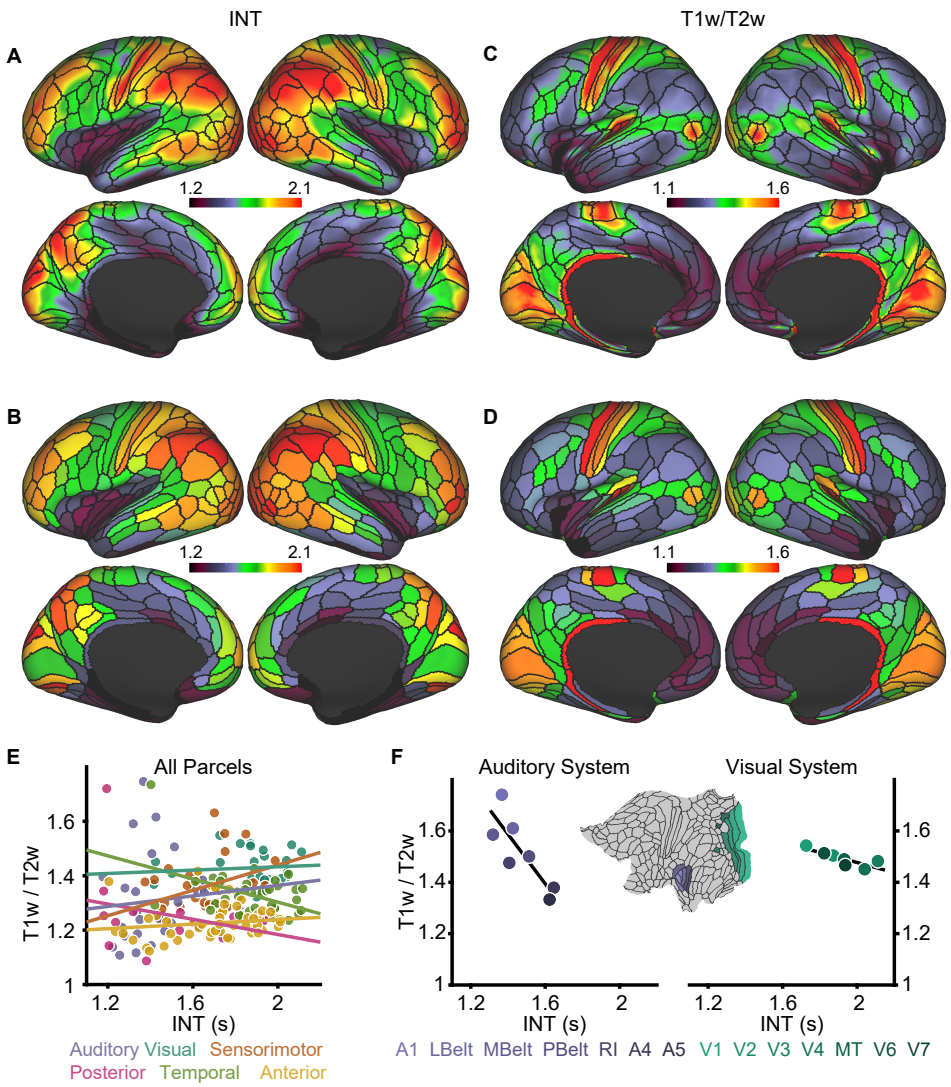

**Figure 1. Relationship between intrinsic neural timescale and T1w/T2w values. A)** Group-averaged intrinsic neural timescale (INT) map ($N = 100$). **B)** Parcellated group-averaged INT map. **C)** Group-averaged T1w/T2w map ($N = 100$). **D)** Parcellated group-averaged T1w/T2w map. Visually, several brain regions with long intrinsic neural timescale show low T1w/T2w map value and vice versa. Additionally, INT values are region-dependent, with little information being lost from parcellation. **E)** Scatterplot showing no consistent relationship between INT and T1w/T2w values across the whole brain, with significant parcel-group interactions (**Supplement**). Data points are parcel-wise means across subjects. **F)** Scatterplots showing strong inverse relationships between INT and T1w/T2w values within the well-defined anatomical hierarchies of the auditory and visual systems. Inset shows the flattened parcellated cortex. Data points are parcel-wise means across subjects.

### *3.2. Assessment of Robustness and Reliability in the HCP Dataset*

Next, we set out to determine the robustness and reliability of the measured INT values. We focused on head motion, a common source of artifacts in fMRI data (37). Head motion during data acquisition was associated with generally decreased INT values (181 out of 188 parcels, $P_{permutation} = 0.01$; **Supplement**). Yet these effects were comparable across hierarchical levels (all $P_{permutation} > 0.31$; **Supplement**). No effects were observed for gender or age (all $P_{permutation} > 0.08$; **Supplement** ). Finally, INT maps showed excellent reliability between the first and last 5 minutes of the fMRI acquisition (median ICC[2,1] $\pm$ interquartile range across voxels: $0.94 \pm 0.03$; **Supplement**).

### *3.3. Exploratory Analysis of Intrinsic Neural Timescales in Schizophrenia versus Health*

Although our primary hypothesis dealt with hierarchical differences between hallucinations and delusions, we first present exploratory analyses of diagnosis effects on INT. Participant characteristics are listed in **Table 1**. Relative to controls, patients exhibited a small-to-moderate but widespread reduction in INT (98 out of 188 parcels, $P_{permutation} = 0.01$; **Figure 2E**). A similar result was observed in a voxel-wise analysis (5,511 out of 27,884 voxels; **Supplement**). The INT reductions in patients were comparable across hierarchical levels (all $P_{permutation} > 0.33$; **Figure 2E-F**). *In silico* simulations using a large-scale biophysical model suggested that the global INT reduction in patients could be neuronally implemented by globally reduced E/I ratio (**Supplement**).

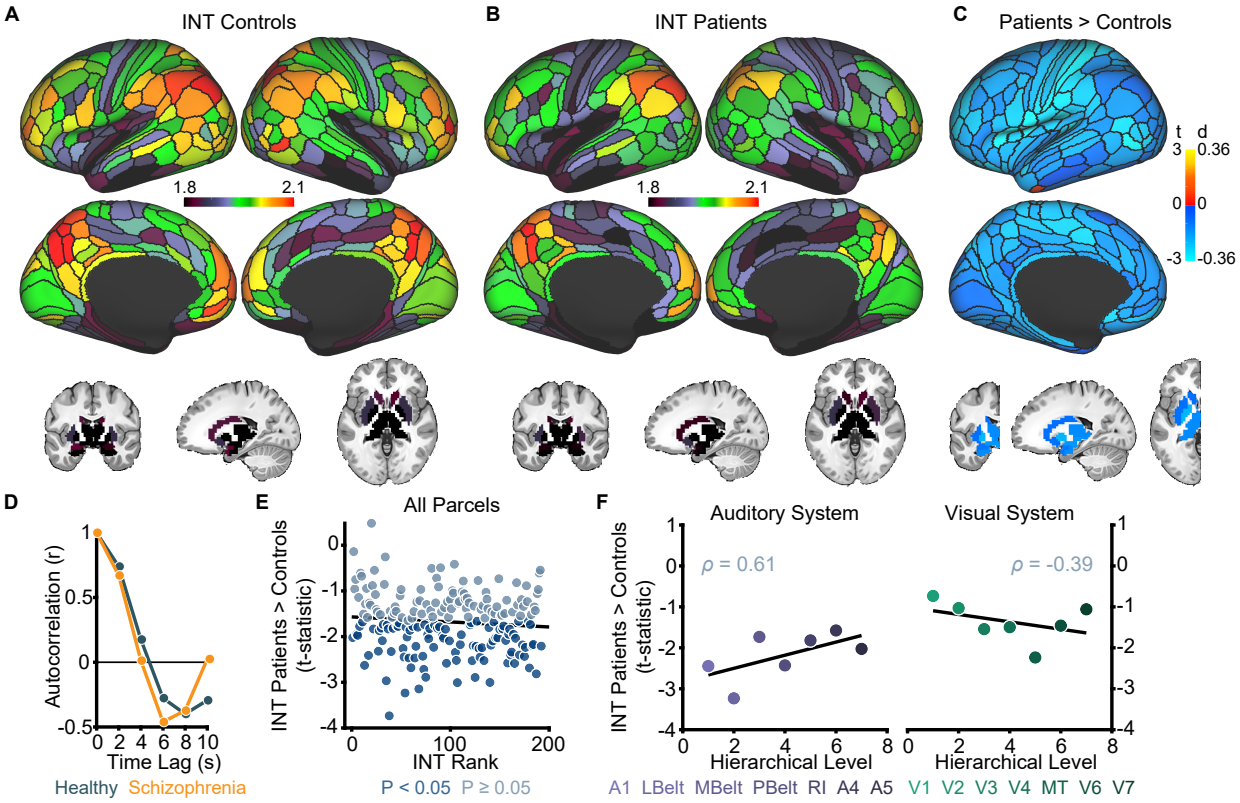

**Figure 2. Patients with schizophrenia show widespread reductions in intrinsic neural timescales compared to healthy controls**. **A)** Parcellated group-averaged intrinsic neural timescale (INT) map for healthy controls (*N* = 158). **B)** Parcellated group-averaged INT map for patients with schizophrenia (*N* = 127). **C)** t-statistic (Cohen's d) map showing the contrast of patients minus controls: across most parcels, INT is smaller in patients than controls when controlling for age, gender, framewise displacement, and data-collection site. Only the left hemisphere is shown because statistical analyses were performed after averaging the values in each parcel across left- and right-hemispheres. **D)** To illustrate the effect of reduced INT in patients with schizophrenia, the group-averaged, whole-brain-averaged autocorrelation functions were estimated from subjects with fMRI data acquired with the same repetition time (Healthy: *N* = 132; Schizophrenia: *N* = 101). The group-averaged autocorrelation function for patients with schizophrenia crosses the zero point on the y axis (i.e., autocorrelation coefficient = 0) sooner than in healthy controls, demonstrating the global reduction of INT in patients with schizophrenia. **E)** Scatterplot showing t-statistic values from a regression model predicting INT group differences controlling for age, gender, framewise displacement and data collection site, plotted as a function of the INT rank (determined from group-averaged INT map from HCP subjects to reduce circularity). Each datapoint represents one parcel. This global INT reduction in patients was not modulated by order within the INT hierarchy over all brain parcels (i.e., the correlation in **E** is not significant against the null distribution). **F)** Scatterplots showing t-statistic values from parcels within the well-defined auditory (left) or visual (right) hierarchy plotted as a function of hierarchical level. The effect of schizophrenia diagnosis on estimated INT was not modulated by position within well-defined sensory hierarchies (i.e., the correlations in **F** are not significant against the null distribution).

### *3.4. Hierarchical Differences in Intrinsic Neural Timescales Between Hallucinations and Delusions*

We hypothesized that hallucinations and delusions were associated with alterations in INT at different hierarchical levels. To test this, we determined the unique

variance associated with the effect of interindividual variability in hallucination and delusion severity on INT. (Exploratory analyses for other symptoms are reported in the **Supplement**.) As expected, severity of hallucinations and delusions in our sample were correlated ($\rho = 0.58$, $P < 0.01$) but exhibited sufficient unique variance [$(1 - R^2) = 0.66$] to evaluate their independent contributions; severity of these symptoms was uncorrelated with antipsychotic dose among the 109 patients with available data (chlorpromazine equivalents: both $P > 0.65$), making it an unlikely confound (**Supplement**).

Critically, we found a significant difference in hierarchical-gradient effects across symptoms (hallucinations and delusions) and sensory systems (symptom-by-hierarchical-level-by-sensory-system interaction: $t_{20} = -3.78$, $P_{permutation} = 0.02$; **Figure 3A**). This interaction was driven by a significant difference for hallucination severity versus delusion severity in the auditory hierarchy (symptom-by-hierarchical-level interaction: $t_{20} = 3.51$, $P_{permutation} = 0.02$; **Figure 3A**) that was non-significant in the visual hierarchy ($t_{20} = -1.83$, $P_{permutation} = 0.20$; **Figure 3A**). Dissecting the interaction within the auditory system showed that patients with more severe hallucinations tended to exhibit a relative increase in INT at lower levels of the auditory hierarchy, leading to a compression of the INT hierarchical gradient (hierarchical-level effect: $t_{20} = -2.63$, $P_{permutation} = 0.07$; **Figure 3**); in contrast, patients with more severe delusions trended towards a relative increase in INT at higher levels of the auditory hierarchy, leading to a more pronounced INT hierarchical gradient (hierarchical-level effect: $t_{20} = 2.34$, $P_{permutation} = 0.11$; **Figure 3**). Post-hoc analyses testing hierarchical-level effects

separately for each symptom and sensory system only showed a significant gradient effect for hallucination-severity within the auditory system ($\rho$ = -0.82, $P_{permutation}$ = 0.04; **Figure 3A**). Thus, we found INT differences between these symptoms along the well-defined anatomical hierarchies of the auditory system, as well as evidence for differences in this effect between the auditory and visual systems. Analyses including the sensorimotor system showed similar results, as well as similar differences by symptom in the hierarchical-gradient effects of the sensorimotor and auditory systems (**Supplement**).

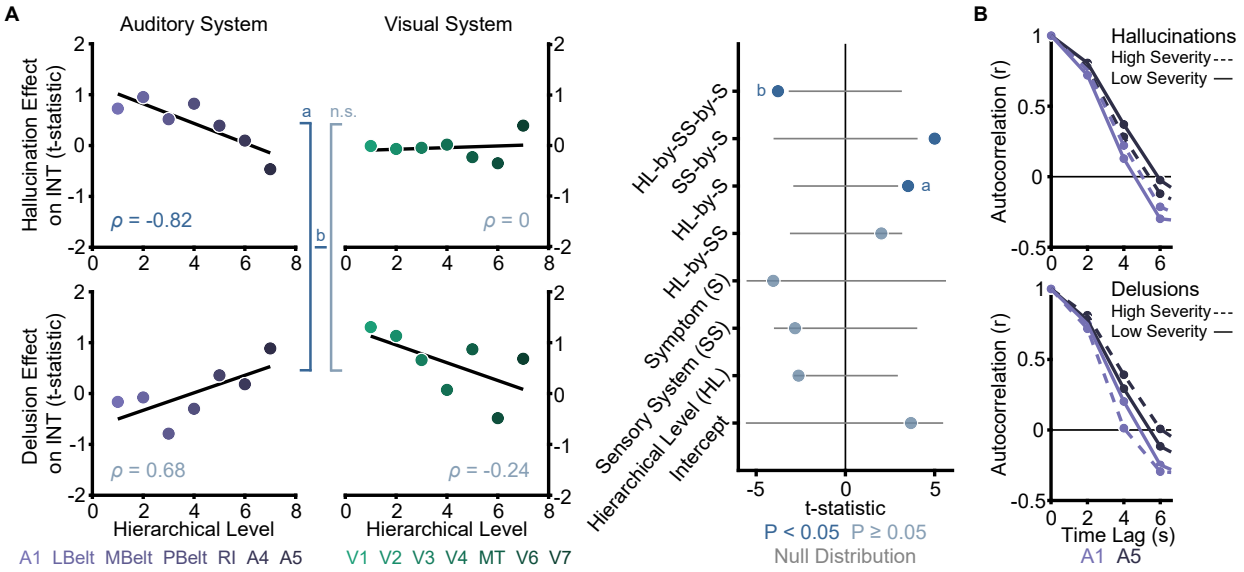


**Figure 3: Hallucinations and delusions show distinct hierarchical-gradient effects in the auditory system. A)** Scatterplots showing t-statistic values for hallucination-severity (top) or delusion-severity (bottom) effects from parcels within the well-defined auditory (left) or visual (center) hierarchies plotted as a function of hierarchical level. Notably, results from a model including symptom-severity effect (hallucination or delusion), hierarchical level, sensory system, and their interactions are shown (right), demonstrating: (1) in the auditory system, a significant difference in the relationship between hallucination severity and hierarchical level versus that for delusion severity and hierarchical level (a) and (2) a

significant 3-way interaction between hierarchical level, sensory system, and symptom (b). **B)** To illustrate the effects, the group-averaged autocorrelation functions were estimated from subjects with fMRI data acquired with the same repetition time. The group-averaged autocorrelation function for patients with high (dashed lines) and low (solid lines) hallucination severity from low and high levels of the auditory hierarchy (A1 and A5, top). The group-averaged autocorrelation function for patients with high (dashed lines) and low (solid lines) delusion severity from A1 and A5 (bottom). High hallucination-severity subjects exhibit a compression of the auditory hierarchical gradient while high delusion-severity subjects exhibit an expansion of this gradient.

*In silico* simulations using a large-scale biophysical model suggested that the observed relationship of hierarchical INT alterations with hallucinations and delusions could be neuronally implemented by elevated E/I ratios at low versus high hierarchical levels, respectively (**Figure 4**).

In exploratory analyses, neither hallucination severity nor delusion severity showed overall changes in INT values (both $P_{permutation} > 0.45$; **Supplement**) or hierarchical-gradient effects over all brain parcels (both $P_{permutation} > 0.39$; **Supplement**). The latter effect did not differ between hallucinations and delusions ($t_{372} = -2.50$, $P_{permutation} = 0.51$; **Supplement**).

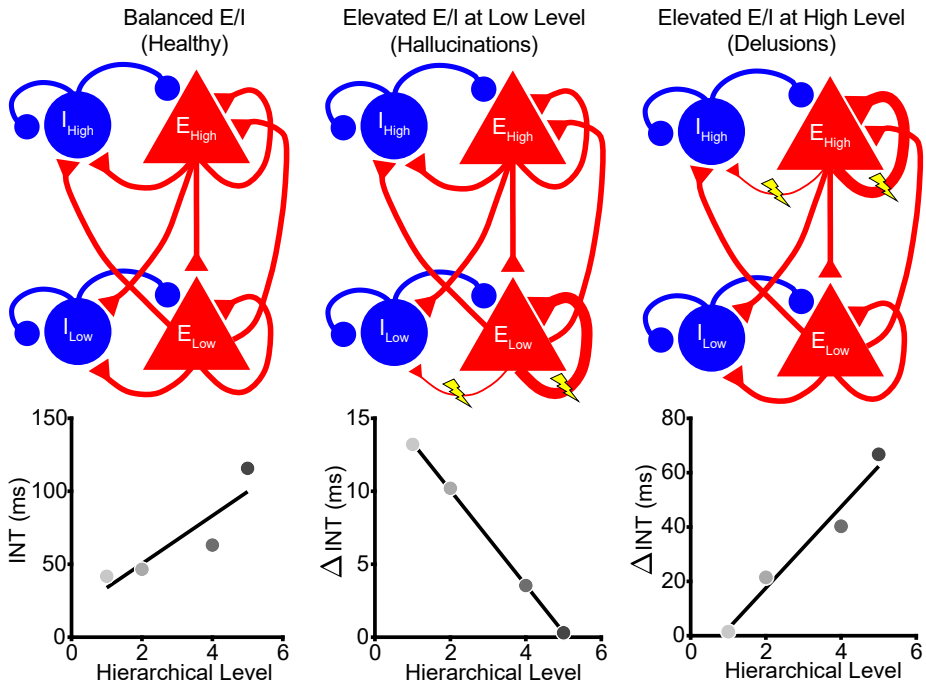


**Figure 4: Hallucination and delusion severity effects are recapitulated by elevated excitatory/inhibitory ratios at different hierarchical levels.** Simulation results from a large-scale biophysical model of primate cortex (Supplement). The model consists of 29 nodes with local excitatory (red triangles) and inhibitory pools (blue circles) of neurons. Only two nodes—high (top) and low (bottom) hierarchical levels—are shown for illustrative purposes. These nodes have both local (recurrent) and long-range (across nodes) connections. The hierarchy within the visual cortex is used for these simulations given lacking tract-tracing data for auditory cortex, but the qualitative pattern of results applies to hierarchical effects in any given sensory system. A scatterplot shows intrinsic neural timescale (INT) values estimated for a reference (healthy) simulated case, which demonstrates the natural hierarchy of timescales (unaltered model; left). Relative to the reference case, increased excitatory-to-excitatory recurrent connection strength or decreased excitatory-to-inhibitory recurrent connection strength (elevated E/I ratio) at the low hierarchical levels leads to increased INT at these levels (middle), emulating the compressed hierarchical gradient related to hallucinations. Relative to the reference case, increased excitatory-to-excitatory recurrent connection strength or decreased excitatory-to-inhibitory recurrent connection strength (elevated E/I ratio) at the high hierarchical levels leads to increased INT at these levels (right), emulating the expanded hierarchical gradient related to delusions. Perturbations to the

model are marked by lightning bolts. Thicker or thinner lines with respect to the reference case reflect increased or decreased connection strengths, respectively.

## 4. Discussion

Using a recently developed method for measuring neural timescales from resting-state fMRI data, we set out to test the hypothesis that hallucinations and delusions are associated with dysfunctions at different levels of neural hierarchies. We first evaluated the relationship between INT and myelin (T1w/T2w) maps, indices of functional and a structural hierarchy, respectively, and demonstrated their convergence albeit only in anatomically defined hierarchies within sensory systems. After further showing excellent reliability of INT measures, in exploratory analyses we showed for the first time that patients with schizophrenia have globally reduced INT. Most importantly, our analyses comparing INT for hallucinations versus delusions demonstrated that these symptoms are associated with distinct changes along the hierarchical gradients in the auditory system, an effect we failed to observe in the visual system.

Hierarchical models of perceptual inference posit that perceptions are shaped by prior beliefs (18, 49-52) through reciprocal message-passing across different levels of sensory-processing hierarchies, the architecture of which mirrors the known anatomy of sensory systems (36, 44-48). In this scheme, higher levels of the neural hierarchy are thought to represent increasingly abstract belief states that evolve at slower timescales (18). For instance, during speech perception, the hierarchical structure of linguistic units can be parsed such that lower levels of auditory processing encode syllable information at faster timescales while higher levels encode sentence information at slower

timescales (53). An emerging body of work in psychosis has linked hallucinations to preferential biases towards prior beliefs in low-level inferences during detection or estimation of stimulus features (5-8) and delusions to preferential biases towards prior beliefs in higher-level inferences about more abstract hidden states (4) (see **Supplement** for related but distinct frameworks).

The observed biases towards prior beliefs in past behavioral work can be framed as primacy biases (4), where past information is weighted more heavily during the inferential process, or equivalently, where information is integrated over longer timescales (27). Temporal integration is at the core of the neural implementation of perceptual inference (28) and is thought to depend crucially on recurrent network activity (16, 29). Thus, a plausible neuronal implementation of primacy biases at a given level of the hierarchy would be through increases in the strength of recurrent excitation or decreases in the strength of recurrent inhibition (i.e., elevated E/I ratio) leading to relative increases in neural timescales.

Here, we observed changes in neural timescales across anatomical levels of the auditory hierarchy that differed between hallucinations and delusions: patients with more severe hallucinations exhibited a less pronounced hierarchical gradient, consistent with increased timescales at lower levels, and those with more severe delusions instead exhibited a more pronounced hierarchical gradient, consistent with increased timescales at higher levels (**Figure 3**). We further recapitulated these findings by respectively elevating E/I ratios at low or high hierarchical levels of a large-scale dynamical model (16). These changes could, in principle, result from alterations in NMDA or dopamine

activation at these levels, in line with glutamatergic or dopaminergic theories of psychosis (11, 54-59). These results thus demonstrate distinct hierarchical alterations for hallucinations and delusions that are generally consistent with our hypothesized hierarchical framework, where distinct hierarchical alterations provide symptom-specific pathways that together may explain symptom co-occurrence (see **Supplement** for predicted data for different symptom profiles), and present a plausible biological mechanism.

Such hierarchical alterations may also fit well with the phenomenological timescale of these symptoms. Clinical observation indicates that hallucinations—like rapidly changing sensory events—change transiently and intermittently over seconds or minutes, while delusions—like slowly changing 'conceptual' beliefs—evolve more slowly over days or months, but their average severity over a given period of time typically evolves in parallel. All these clinical features are consistent with a hierarchical structure of nested timescales (17). While our findings generally support this notion, computational work explicitly laying out the proposed model in the context of inferential alterations in psychosis and empirical confirmations are warranted.

Our opposing findings for diagnosis (globally reduced INT) and symptom severity (focally increased INT) may be reconciled within pathophysiological models of psychosis which posit a key role for compensatory processes in schizophrenia. Hallucinations and delusions have been proposed to represent a temporary state of the illness that results from a failed attempt to compensate for a trait-like, baseline deficit (3, 60). Relatedly, long-standing circuit-level theories have suggested that psychosis-

related increases in striatal dopamine transmission is secondary to a primary cortical deficit (61). In particular, previous frameworks suggest that psychotic states are associated with excessive prior biases in inferential processes arising as an overcompensation for a baseline trait consisting of the opposite bias (2, 3). From a biophysical-modeling standpoint, the trait-like baseline deficit in schizophrenia could consist of reduced E/I ratio (for instance, arising from NMDA-receptor hypofunction of excitatory neurons (62)), which behaviorally would translate into general recency biases. In contrast, a failed compensatory mechanism could result in local increases in E/I ratio at different levels leading to distinct primacy biases and psychotic symptoms (63). While speculative, the compensatory changes could arise from dopaminergic alterations that effectively increase E/I ratio by preferentially boosting NMDA-receptor function of excitatory neurons (or other changes dampening NMDA-receptor function of inhibitory neurons) (55).

Our finding of a preferential involvement of the auditory system may be unsurprising for hallucinations, since in schizophrenia this symptom tends to predominate in the auditory modality despite also presenting in the visual and other modalities (41, 42). But the reason for the differences in the auditory hierarchy involving delusions is unclear. The mounting evidence of auditory-cortex abnormalities in schizophrenia (64) could suggest that delusions originate from auditory-cortex dysfunctions despite their modality-unspecific nature. Nonetheless, substantial evidence also suggests visual-cortex abnormalities in schizophrenia (65-67) and evidence from subclinical populations suggests symptom-specific hierarchical alterations in visual

tasks (6). Furthermore, the general differences in INT values between the auditory and visual system (**Figure 1**), while potentially relevant to psychosis in and of themselves, could imply differential sensitivity in our analyses across sensory domains. Furthermore, our supplemental results involving the sensorimotor system, consistent with prior work (68, 69), suggest psychosis-relevant alterations that are not limited to the auditory system.

Previous empirical work using structural (70) and functional measures (71-73), suggests hierarchical alterations in schizophrenia. This work however did not evaluate hierarchical differences between symptoms and used measures that differ fundamentally from our INT measure. In exploratory analyses testing diagnostic effects, we found global INT decreases in schizophrenia but failed to detect any general shifts in the hierarchical INT gradients. We used the same approach as a previous study measuring INT in individuals with autism, which reported decreased INT in visual cortex (and increased INT in the caudate) (26). Consistent with our interpretation, this INT phenotype was linked to other data in autism supporting excessive weighting of sensory evidence (74, 75)—akin to a decreased primacy bias, or a recency bias.

Some limitations are worth discussing. Because 93% of the patients (with available medication data) were taking antipsychotics, we cannot definitively rule out medication confounds, particularly on diagnosis effects. However, we observed no dose effects and no correlations between dose and symptoms, and did not expect differential neural modulations for hallucinations versus delusions (**Supplement**). Future studies should elucidate the effect of antipsychotics, and dopamine manipulations more

generally, on INT. Lastly, we decided to focus on well-defined anatomical hierarchies within the auditory and visual systems, rather than including higher-level regions beyond associative sensory cortex (e.g., dorsolateral prefrontal cortex). This was justified by the ambiguity associated with defining hierarchical levels for the highest-level regions (76, 77) and because, when excluded, hierarchies within sensory regions alone still span roughly 75% of the entire hierarchical range (16, 78). Moreover, our results held when we added the dorsolateral prefrontal cortex in the analysis as the top level in the hierarchy (**Supplement**).

In conclusion, we have presented neural evidence for distinct hierarchical changes in neural timescales in the auditory cortex as a function of hallucination and delusion severity, lending initial support for hierarchical views of psychosis. Additionally, our work suggests that INT (26) provides a reliable and interpretable measure of neural function with potential to elucidate hierarchical alterations and dysfunctions in circuit dynamics in schizophrenia and other neuropsychiatric disorders.

## 5. Acknowledgments

The authors would like to thank Drs. Rishidev Chaudhuri and Xiao-Jing Wang for their guidance in implementing the large-scale biophysical model. This work was supported by the National Institute of Mental Health under awards R01MH117323 and R01MH114965. BrainGluSchi: data were downloaded from the COllaborative Informatics and Neuroimaging Suite Data Exchange tool (COINS;http://coins.mrn.org/dx) and data collection was funded by NIMH

R01MH084898-01A1. COBRE: Data was downloaded from the COllaborative Informatics and Neuroimaging Suite Data Exchange tool (COINS; http://coins.mrn.org/dx), data collection was performed at the Mind Research Network, and funded by a Center of Biomedical Research Excellence (COBRE) grant 5P20RR021938/P20GM103472 from the NIH to Dr. Vince Calhoun. NMorphCH: data were obtained from the Neuromorphometry by Computer Algorithm Chicago (NMorphCH) dataset (http://nunda.northwestern.edu/nunda/data/projects/NMorphCH); the investigators within NMorphCH contributed to the design and implementation of NMorphCH and/or provided data but did not participate in analysis or writing of this report; data collection and sharing for this project was funded by NIMH grant R01MH056584. UCLA: data was obtained from the OpenfMRI database (its accession number is ds000030) and data collection was funded by the Consortium for Neuropsychiatric Phenomics (NIH Roadmap for Medical Research grants UL1-DE019580, RL1MH083268, RL1MH083269, RL1DA024853, RL1MH083270, RL1LM009833, PL1MH083271, and PL1NS062410). HCP: Data were provided by the Human Connectome Project, WU-Minn Consortium (Principal Investigators: David Van Essen and Kamil Ugurbil; 1U54MH091657) funded by the 16 NIH Institutes and Centers that support the NIH Blueprint for Neuroscience Research; and by the McDonnell Center for Systems Neuroscience at Washington University.

## References

1. P. Sterzer *et al.*, The predictive coding account of psychosis. *Biological psychiatry* **84**, 634-643 (2018).

2. G. Horga, A. Abi-Dargham, An integrative framework for perceptual disturbances in psychosis. *Nature Reviews Neuroscience*, 1-16 (2019).

3. R. A. Adams, K. E. Stephan, H. R. Brown, C. D. Frith, K. J. Friston, The computational anatomy of psychosis. *Frontiers in psychiatry* **4**, 47 (2013).

4. S. C. Baker, A. B. Konova, N. D. Daw, G. Horga, A distinct inferential mechanism for delusions in schizophrenia. *Brain* **142**, 1797-1812 (2019).

5. C. M. Cassidy *et al.*, A perceptual inference mechanism for hallucinations linked to striatal dopamine. *Current Biology* **28**, 503-514. e504 (2018).

6. D. J. Davies, C. Teufel, P. C. Fletcher, Anomalous perceptions and beliefs are associated with shifts toward different types of prior knowledge in perceptual inference. *Schizophrenia bulletin* **44**, 1245-1253 (2017).

7. C. Teufel *et al.*, Shift toward prior knowledge confers a perceptual advantage in early psychosis and psychosis-prone healthy individuals. *Proceedings of the National Academy of Sciences* **112**, 13401-13406 (2015).

8. A. R. Powers, C. Mathys, P. Corlett, Pavlovian conditioning–induced hallucinations result from overweighting of perceptual priors. *Science* **357**, 596-600 (2017).

9. R. A. Adams, G. Napier, J. P. Roiser, C. Mathys, J. Gilleen, Attractor-like dynamics in belief updating in schizophrenia. *Journal of Neuroscience* **38**, 9471-9485 (2018).

10. P. C. Fletcher, C. D. Frith, Perceiving is believing: a Bayesian approach to explaining the positive symptoms of schizophrenia. *Nature Reviews Neuroscience* **10**, 48 (2009).

11. P. R. Corlett, C. D. Frith, P. C. Fletcher, From drugs to deprivation: a Bayesian framework for understanding models of psychosis. *Psychopharmacology* **206**, 515-530 (2009).

12. P. R. Corlett *et al.*, Hallucinations and strong priors. *Trends in cognitive sciences* (2018).

13. A. R. Powers III, M. Kelley, P. R. Corlett, Hallucinations as top-down effects on perception. *Biological Psychiatry: Cognitive Neuroscience and Neuroimaging* **1**, 393-400 (2016).

14. P. R. Corlett, J. H. Krystal, J. R. Taylor, P. C. Fletcher, Why do delusions persist? *Frontiers in human neuroscience* **3**, 12 (2009).

15. K. Schmack *et al.*, Delusions and the role of beliefs in perceptual inference. *Journal of Neuroscience* **33**, 13701-13712 (2013).

16. R. Chaudhuri, K. Knoblauch, M.-A. Gariel, H. Kennedy, X.-J. Wang, A large-scale circuit mechanism for hierarchical dynamical processing in the primate cortex. *Neuron* **88**, 419-431 (2015).

17. S. J. Kiebel, J. Daunizeau, K. J. Friston, A hierarchy of time-scales and the brain. *PLoS computational biology* **4**, e1000209 (2008).

18. S. J. Kiebel, J. Daunizeau, K. J. Friston, Perception and hierarchical dynamics. *Frontiers in neuroinformatics* **3**, 20 (2009).

19. G. Major, D. Tank, Persistent neural activity: prevalence and mechanisms. *Current opinion in neurobiology* **14**, 675-684 (2004).

20. J. D. Murray *et al.*, A hierarchy of intrinsic timescales across primate cortex. *Nature neuroscience* **17**, 1661 (2014).

21. U. Hasson, J. Chen, C. J. Honey, Hierarchical process memory: memory as an integral component of information processing. *Trends in cognitive sciences* **19**, 304-313 (2015).

22. U. Hasson, E. Yang, I. Vallines, D. J. Heeger, N. Rubin, A hierarchy of temporal receptive windows in human cortex. *Journal of Neuroscience* **28**, 2539-2550 (2008).

23. C. J. Honey *et al.*, Slow cortical dynamics and the accumulation of information over long timescales. *Neuron* **76**, 423-434 (2012).

24. Y. Lerner, C. J. Honey, L. J. Silbert, U. Hasson, Topographic mapping of a hierarchy of temporal receptive windows using a narrated story. *Journal of Neuroscience* **31**, 2906-2915 (2011).

25. G. J. Stephens, C. J. Honey, U. Hasson, A place for time: the spatiotemporal structure of neural dynamics during natural audition. *Journal of neurophysiology* **110**, 2019-2026 (2013).

26. T. Watanabe, G. Rees, N. Masuda, Atypical intrinsic neural timescale in autism. *Elife* **8**, e42256 (2019).

27. C. M. Glaze, J. W. Kable, J. I. Gold, Normative evidence accumulation in unpredictable environments. *Elife* **4**, e08825 (2015).

28. M. E. Mazurek, J. D. Roitman, J. Ditterich, M. N. Shadlen, A role for neural integrators in perceptual decision making. *Cerebral cortex* **13**, 1257-1269 (2003).

29. V. Mante, D. Sussillo, K. V. Shenoy, W. T. Newsome, Context-dependent computation by recurrent dynamics in prefrontal cortex. *nature* **503**, 78 (2013).

30. D. C. Van Essen *et al.*, The WU-Minn human connectome project: an overview. *Neuroimage* **80**, 62-79 (2013).

31. M. F. Glasser, D. C. Van Essen, Mapping human cortical areas in vivo based on myelin content as revealed by T1-and T2-weighted MRI. *Journal of Neuroscience* **31**, 11597-11616 (2011).

32. S. R. Kay, A. Fiszbein, L. A. Opler, The positive and negative syndrome scale (PANSS) for schizophrenia. *Schizophrenia bulletin* **13**, 261-276 (1987).

33. N. C. Andreasen, *Scale for the Assessment of Positive Symptons:(SAPS)* (University of Iowa, 1984).

34. N. Andreasen, The scale for the assessment of negative symptoms (SANS) Iowa City. *IA: University of Iowa* (1983).

35. J. B. Burt *et al.*, Hierarchy of transcriptomic specialization across human cortex captured by structural neuroimaging topography. *Nature neuroscience* **21**, 1251 (2018).

36. M. F. Glasser *et al.*, A multi-modal parcellation of human cerebral cortex. *Nature* **536**, 171 (2016).

37. J. D. Power, K. A. Barnes, A. Z. Snyder, B. L. Schlaggar, S. E. Petersen, Spurious but systematic correlations in functional connectivity MRI networks arise from subject motion. *Neuroimage* **59**, 2142-2154 (2012).

38. P. E. Shrout, J. L. Fleiss, Intraclass correlations: uses in assessing rater reliability. *Psychological bulletin* **86**, 420 (1979).

39. B. Fischl, FreeSurfer. *Neuroimage* **62**, 774-781 (2012).

40. A. Eklund, T. E. Nichols, H. Knutsson, Cluster failure: Why fMRI inferences for spatial extent have inflated false-positive rates. *Proceedings of the national academy of sciences* **113**, 7900-7905 (2016).

41. A. Lim *et al.*, Prevalence and classification of hallucinations in multiple sensory modalities in schizophrenia spectrum disorders. *Schizophrenia research* **176**, 493-499 (2016).

42. F. Waters, C. Fernyhough, Hallucinations: a systematic review of points of similarity and difference across diagnostic classes. *Schizophrenia bulletin* **43**, 32-43 (2017).

43. B. Vázquez-Rodríguez *et al.*, Gradients of structure–function tethering across neocortex. *Proceedings of the National Academy of Sciences* **116**, 21219-21227 (2019).

44. D. J. Felleman, D. E. Van, Distributed hierarchical processing in the primate cerebral cortex. *Cerebral cortex (New York, NY: 1991)* **1**, 1-47 (1991).

45. D. C. Van Essen, C. H. Anderson, D. J. Felleman, Information processing in the primate visual system: an integrated systems perspective. *Science* **255**, 419-423 (1992).

46. J. H. Kaas, T. A. Hackett, Subdivisions of auditory cortex and processing streams in primates. *Proceedings of the National Academy of Sciences* **97**, 11793-11799 (2000).

47. N. T. Markov *et al.*, A weighted and directed interareal connectivity matrix for macaque cerebral cortex. *Cerebral cortex* **24**, 17-36 (2012).

48. M. P. Young, The organization of neural systems in the primate cerebral cortex. *Proceedings of the Royal Society of London. Series B: Biological Sciences* **252**, 13-18 (1993).

49. K. Friston, S. Kiebel, Predictive coding under the free-energy principle. *Philosophical Transactions of the Royal Society B: Biological Sciences* **364**, 1211-1221 (2009).

50. R. P. Rao, D. H. Ballard, Predictive coding in the visual cortex: a functional interpretation of some extra-classical receptive-field effects. *Nature neuroscience* **2**, 79 (1999).

51. P. Dayan, G. E. Hinton, R. M. Neal, R. S. Zemel, The helmholtz machine. *Neural computation* **7**, 889-904 (1995).

52. T. S. Lee, D. Mumford, Hierarchical Bayesian inference in the visual cortex. *JOSA A* **20**, 1434-1448 (2003).

53. N. Ding, L. Melloni, H. Zhang, X. Tian, D. Poeppel, Cortical tracking of hierarchical linguistic structures in connected speech. *Nature neuroscience* **19**, 158 (2016).

54. J. J. Weinstein *et al.*, Pathway-specific dopamine abnormalities in schizophrenia. *Biological psychiatry* **81**, 31-42 (2017).

55. N. Brunel, X.-J. Wang, Effects of neuromodulation in a cortical network model of object working memory dominated by recurrent inhibition. *Journal of computational neuroscience* **11**, 63-85 (2001).

56. D. Durstewitz, J. K. Seamans, The computational role of dopamine D1 receptors in working memory. *Neural Networks* **15**, 561-572 (2002).

57. R. Jardri *et al.*, Are hallucinations due to an imbalance between excitatory and inhibitory influences on the brain? *Schizophrenia bulletin* **42**, 1124-1134 (2016).

58. D. C. Javitt, S. R. Zukin, U. Heresco-Levy, D. Umbricht, Has an angel shown the way? Etiological and therapeutic implications of the PCP/NMDA model of schizophrenia. *Schizophrenia bulletin* **38**, 958-966 (2012).

59. P. R. Corlett, G. D. Honey, J. H. Krystal, P. C. Fletcher, Glutamatergic model psychoses: prediction error, learning, and inference. *Neuropsychopharmacology* **36**, 294 (2011).

60. M. Moutoussis, R. P. Bentall, W. El-Deredy, P. Dayan, Bayesian modelling of Jumping-to-Conclusions bias in delusional patients. *Cognitive neuropsychiatry* **16**, 422-447 (2011).

61. D. R. Weinberger, Implications of normal brain development for the pathogenesis of schizophrenia. *Archives of general psychiatry* **44**, 660-669 (1987).

62. S. E. Cavanagh, N. H. Lam, J. D. Murray, L. T. Hunt, S. W. Kennerley, A circuit mechanism for irrationalities in decision-making and NMDA receptor hypofunction: behaviour, computational modelling, and pharmacology. *bioRxiv*, 826214 (2019).

63. N. H. Lam *et al.*, Effects of altered excitation-inhibition balance on decision making in a cortical circuit model. *bioRxiv*, 100347 (2017).

64. D. C. Javitt, R. A. Sweet, Auditory dysfunction in schizophrenia: integrating clinical and basic features. *Nature Reviews Neuroscience* **16**, 535-550 (2015).

65. P. D. Butler, S. M. Silverstein, S. C. Dakin, Visual perception and its impairment in schizophrenia. *Biological psychiatry* **64**, 40-47 (2008).

66. I. Çavuş *et al.*, Impaired visual cortical plasticity in schizophrenia. *Biological psychiatry* **71**, 512-520 (2012).

67. K. A. Dorph-Petersen, J. N. Pierri, Q. Wu, A. R. Sampson, D. A. Lewis, Primary visual cortex volume and total neuron number are reduced in schizophrenia. *Journal of comparative neurology* **501**, 290-301 (2007).

68. S. S. Shergill *et al.*, Functional magnetic resonance imaging of impaired sensory prediction in schizophrenia. *JAMA psychiatry* **71**, 28-35 (2014).

69. S. S. Shergill, G. Samson, P. M. Bays, C. D. Frith, D. M. Wolpert, Evidence for sensory prediction deficits in schizophrenia. *American Journal of Psychiatry* **162**, 2384-2386 (2005).

70. D. S. Bassett *et al.*, Hierarchical organization of human cortical networks in health and schizophrenia. *Journal of Neuroscience* **28**, 9239-9248 (2008).

71. D. I. Leitman *et al.*, Sensory deficits and distributed hierarchical dysfunction in schizophrenia. *American Journal of Psychiatry* **167**, 818-827 (2010).

72. G. J. Yang *et al.*, Functional hierarchy underlies preferential connectivity disturbances in schizophrenia. *Proceedings of the National Academy of Sciences* **113**, E219-E228 (2016).

73. C. Dondé, G. Silipo, E. C. Dias, D. C. Javitt, Hierarchical deficits in auditory information processing in schizophrenia. *Schizophrenia research* **206**, 135-141 (2019).

74. R. P. Lawson, C. Mathys, G. Rees, Adults with autism overestimate the volatility of the sensory environment. *Nature neuroscience* **20**, 1293 (2017).

75. L. L. Gollo, Computational Psychiatry: Exploring atypical timescales in the brain. *eLife* **8**, e45089 (2019).

76. C.-C. Hilgetag, D. C. Van Essen, M. A. O'Neill, M. P. Young, D. J. Felleman, Indeterminate organization of the visual systemon hierarchies: Response to hilgetag et al. rejoinder: Further commentary: Determinate or indeterminate organization. *Science* **271**, 776-776 (1996).

77. C. C. Hilgetag, M. A. O'Neill, M. P. Young, Hierarchical organization of macaque and cat cortical sensory systems explored with a novel network processor. *Philosophical Transactions of the Royal Society of London. Series B: Biological Sciences* **355**, 71-89 (2000).

78. N. T. Markov *et al.*, Anatomy of hierarchy: feedforward and feedback pathways in macaque visual cortex. *Journal of Comparative Neurology* **522**, 225-259 (2014).